Progress In Electromagnetics Research M, Vol. 67, 65–73, 2018

Compact CPW-Fed Circularly Polarized Antenna for WLAN Application

Manas Midya*, Shankar Bhattacharjee, and Monojit Mitra

Abstract—A novel compact CPW (coplanar waveguide-fed) CPSS (Circularly polarized square slot) antenna is presented. The proposed single-layer antenna is composed of a rectangular ground plane embedded with two equal-size patches along two orthogonal directions. Equal amplitudes with 90° phase difference values of two patches are capable of generating a resonant mode for exciting two orthogonal E vectors. Axial ratio (AR) bandwidth is significantly enhanced due to slot corner modification. The designed CPSS antenna is compact in nature with volume of $0.37\lambda_0 \times 0.34\lambda_0 \times 0.012\lambda_0\,\text{mm}^3$ (λ_0 = free space wavelength at centre frequency of the CP bandwidth). It has impedance bandwidth between 4.65–6.72 GHz (36.41%) and 3-dB axial-ratio bandwidth of 520 MHz (4.85–5.37 GHz), which covers 4.9 GHz (802.11j) WLAN for public safety ranging from 4.94 GHz to 4.99 GHz and WLAN (U-NII-1 and U-NII-2A) ranging from 5.150–5.350 GHz for indoor use. The gain variation for the frequencies within the CP bandwidth is also observed to be less than 0.4 dBic. The design is successfully implemented, and measured results are compared with the simulated ones, which are found good agreement.

1. INTRODUCTION

Circularly polarized (CP) antenna is widely popular for wireless communication due to its capability of preventing polarization mismatch, multipath interference and flexibility in the orientation angle between transmitting and receiving antennas [1]. Circular polarization is achieved when antenna radiates two orthogonal electric field vectors with equal amplitude and in-phase quadrature are excited [2]. Due to the advantage of low profile and easy fabrication technique of slot antenna, it is preferable for realization of CP operations. Narrow AR bandwidth limits the application of Broadband CP application. To overcome the problem of narrow impedance and axial-ratio bandwidths (ARBWs), various shapes and designs have been proposed [3–6]. However, narrow CP band antenna is preferable for some wireless communication bands [7–10].

Circularly polarized antenna can be achieved by using various types of feeding methods: CPW-fed [11], microstrip line fed [12–14], inset fed and using mutual coupling [15, 16], aperture couple [17] etc.. However these types of feeding techniques can be used in two ways: single-fed and dual-fed. The "self phased" concept is usually used for single-fed CP radiation. The major advantage of single-fed CP antenna is their simple structure and it does not need any external phase shifter. Various techniques and configurations for CP antennas have been investigated and reported using single-fed configuration. Various techniques of this configuration includes embedding a pair of inverted-L-shaped strips around two opposite corners of the square slot [18], impedance matching stub and a cross-shaped radiating patch together with a strip line between two opposite corners of the ground [19], cross slot antenna with an ellipse-shaped ground plane [20], protruding metallic mono-strip from the circular ground plane towards the slot centre at $\varphi = 0°$ [21], single-layered square patch integrated with a novel Y-shaped slot

Received 15 February 2018, Accepted 24 March 2018, Scheduled 6 April 2018

* Corresponding author: Manas Midya (letsmanas@gmail.com).

The authors are with the Department of Electronics & Telecommunication Engineering, Indian Institute of Engineering Science & Technology, Shibpur, India.

and two different truncated corners [22], two orthogonal microstrip lines to feed a single element DRA for obtaining circular polarization [23].

Inspired by previous investigations on CP antennas, a new wideband CPW-fed compact CP antenna is proposed. Two CP modes are produced by two orthogonal patches connected by optimized $\lambda_0/4$ microstrip line using power divider technique. Modified slot at the lower left corner of the square slot is introduced for improving axial ratio bandwidth. The structure is compact, simple, and easy to fabricate. Details of the antenna design is described, and measured results are presented and discussed. High frequency structure simulator (HFSS-14) based on finite element method (FEM) is used to design and optimize the proposed structure. According to authors' knowledge, this is the first CPW-fed compact single layer CP slot antenna using power divider technique with improved CP bandwidth.

2. ANTENNA DESIGN AND ANALYSIS

Top view and side view of the proposed structure are shown in Figure 1. The antenna is printed on an FR-4 substrate with a relative permittivity of 4.4, substrate thickness of 0.74 mm and loss tangent (δ), $0.02 \leq \delta \leq 0.03$ within 12 GHz [24]. It is fed by a $Z = 50\,\Omega$ CPW feed having 2.8 mm wide signal line and two identical gaps of 0.3 mm. The size of the ground plane of this compact CPW-fed slot antenna is $0.37\lambda_0 \times 0.34\lambda_0\,\text{mm}^2$. It has a square slot with modified corner at the left-bottom of the square slot and two orthogonal equal size patches connected by quarter wavelength microstrip line. Power divider is used to distribute equal power (3-dB) on both patches and maintains optimized $\lambda_0/4$ length difference between two microstrip lines to get 90° phase difference. Once the signal is applied at 50 Ω CPW feed line, it is divided into two equal impedance ($Z_1 = Z_2$) microstrip lines having width of 0.8 mm. Microstrip feed lines are connected asymmetrically with the orthogonal patches to obtain better circular polarization. Left-bottom corner of the slot is modified to enhance the CP bandwidth of the proposed antenna up to 220 MHz. The length of each shorter side branch of the patch is 1.6 mm, and total length and width are S_l and S_w, respectively. Slot size of the proposed antenna is $G_l \times G_w\,\text{mm}^2$.

$$Z_1 = Z_2 = Z_0\sqrt{2} = 70.71\,\Omega$$

Steps of improvement for the proposed structure of antenna are described by four prototypes in Figure 2. Their performances are shown in Figure 3 and Figure 4 as well. The proposed antenna

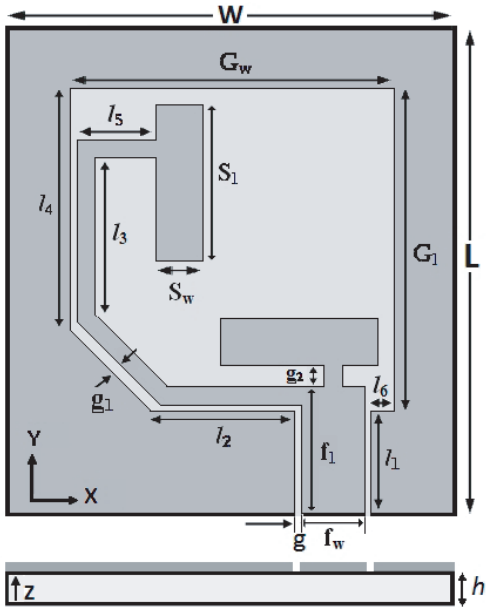

Figure 1. Top and Side view of the antenna. ($W = 20$, $L = 21.8$, $G_l = 14.4$, $G_w = 14.4$, $S_l = 7$, $S_w = 2.1$, $f_1 = 5.7$, $f_w = 2.8$, $l_1 = 4.6$, $l_2 = 6.4$, $l_3 = 6.96$, $l_4 = 10.79$, $l_5 = 3.5$, $l_6 = 1$, $g = 0.3$, $g_1 = 0.5$, $g_2 = 0.93$) (unit: millimeters).

has resonating frequency at 6.3 GHz. Four prototypes (ant 1–4) have been implemented, and their performances are listed in Table 1 for comparison. According to results of Ant (1–4) in Table 1, Figure 3 and Figure 4, maximum impedance and CP bandwidth are obtained for Ant 4 configuration.

Table 1. Antenna performances of constructed prototypes.

	Bandwidth (MHz)	Axial Ratio Bandwidth (MHz)
Ant. 1	No Matching	No
Ant. 2	No Matching	No
Ant. 3	1960	300
Ant. 4	2070	520

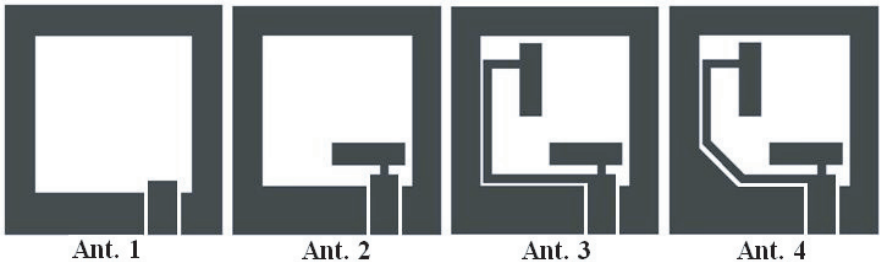

Figure 2. Evolution steps of the antenna.

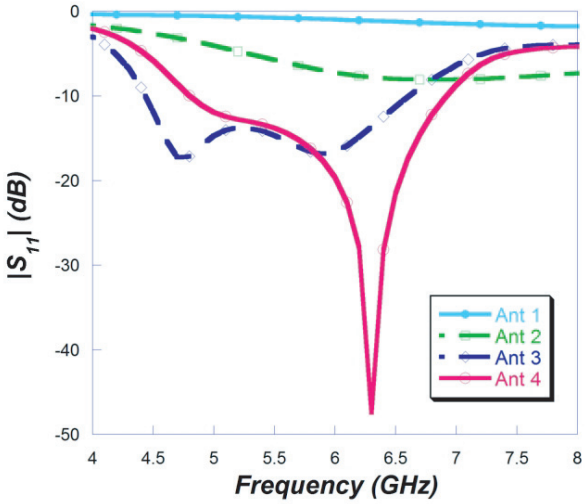

Figure 3. Simulated S_{11} values for different prototypes.

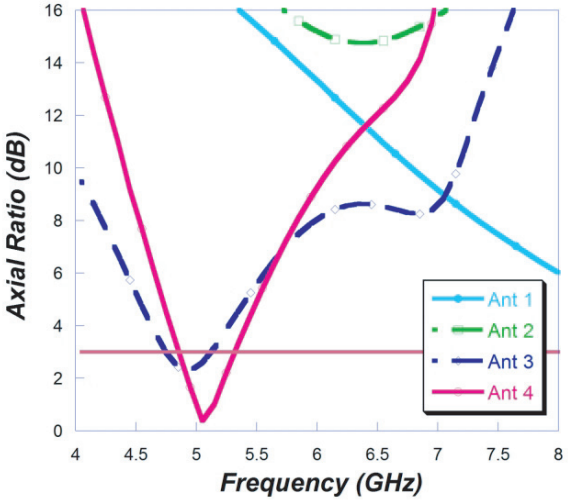

Figure 4. Simulated axial ratio plots for different prototypes.

In order to study the working mechanism of the proposed antenna, several vital parameters are analyzed. Patch length and microstrip-line length are found to play important roles in the CP property of the antenna. Actually both patch length and microstrip-line length affect the resonant frequency of two orthogonal modes, not only the amplitude property but also the phase value. By optimizing the patch length and microstrip-line length, two orthogonal modes are generated with equal amplitude and 90° phase difference, thus CP bandwidth is obtained. To study the effects of various sections on antenna performance parametric analysis has been performed.

2.1. Effect of Rectangular Patch Length (S_l)

With the variation of rectangular patch length, Figure 5 shows that the resonating frequency is inversely proportional to the patch length. As we increase the patch length, resonating frequency is shifted towards lower frequency ($f_r = C/4L\sqrt{\in_r}$), and maximum AR bandwidth is well obtained (Shown in Figure 5 and Figure 6) for $S_l = 7\,\text{mm}$.

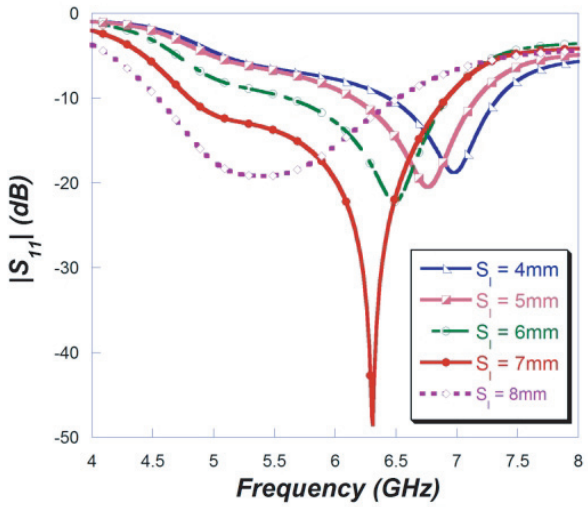

Figure 5. Effect of patch length on the S_{11} values.

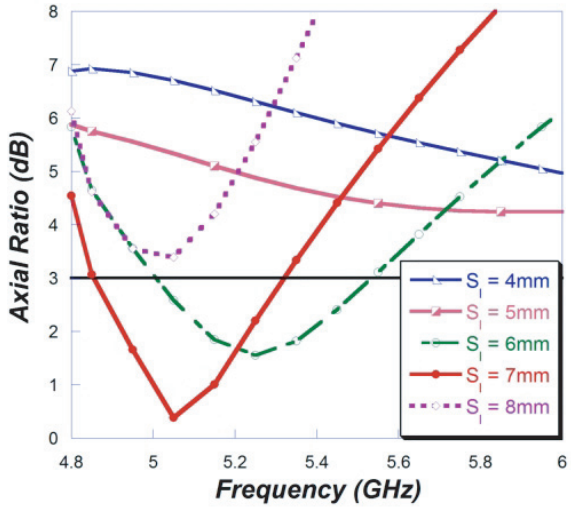

Figure 6. Effect of patch length on the axial ratio values.

2.2. Effect of Microstrip Feed Length (F_l)

Microstrip feed length plays an important role in AR bandwidth, as well as in the resonating frequency of the antenna. As we increase the microstrip feed length, the resonant frequency is shifted towards lower frequency, and maximum AR bandwidth is obtained for $F_l = 20\,\text{mm}$, shown in Figure 7 and Figure 8 as well.

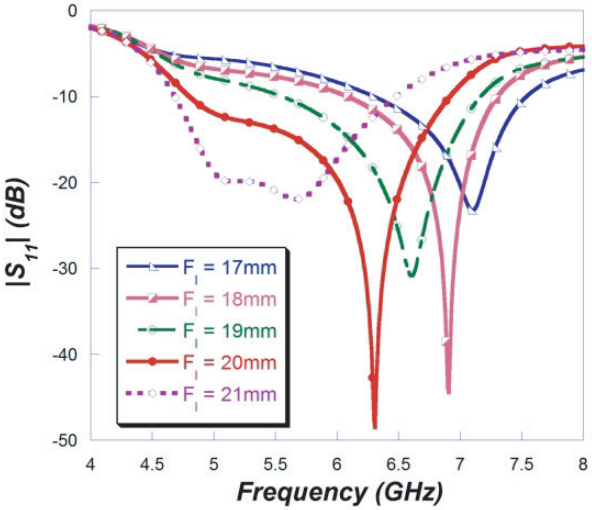

Figure 7. Effect of micro strip line length on the S_{11} values.

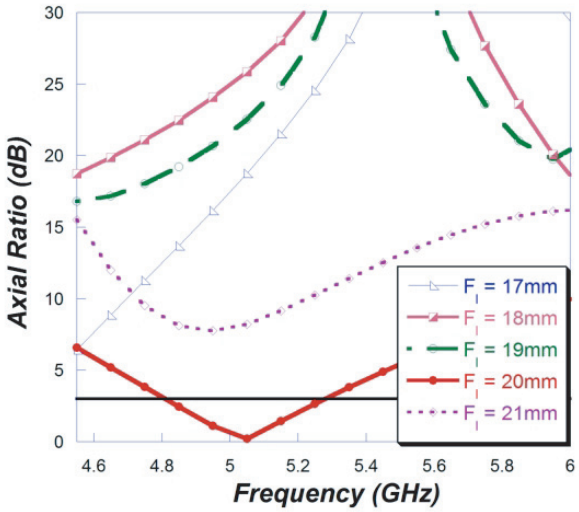

Figure 8. Effect of micro strip line length on the axial ratio value.

Table 2 shows the comparison between the recently published works in open literature and the antenna proposed here. It shows that the proposed antenna is much smaller than that of the recently published work.

Table 2. Performance comparison of proposed antenna antenna with existing CP antennas.

Ref.	Impedance Bandwidth (MHz)	CP centre frequency (MHz)	3 dB AR Bandwidth (MHz)	Antenna size (mm × mm)
[8]	600	4640	100	$0.62\lambda_0 \times 0.62\lambda_0$
[10]	900	3700	500	$0.94\lambda_0 \times 0.94\lambda_0$
[15]	350	5800	151	not shown
[25]	3000	5450	700	$0.45\lambda_0 \times 0.45\lambda_0$
[26]	3650	3625	2450	$0.70\lambda_0 \times 0.70\lambda_0$
[27]	3000	3675	1850	$0.74\lambda_0 \times 0.74\lambda_0$
Proposed	2070	5050	520	$0.37\lambda_0 \times 0.34\lambda_0$

3. EXPERIMENTAL RESULTS AND DISCUSSION

Experimental result shows that the CP operation bandwidth (4.85–5.37 GHz) can be totally covered by the impedance bandwidth (IBW), referred to −10 dB return loss. According to current distribution in Figure 9, the polarization senses are right-handed circular polarization and left-handed circular polarization for $Z > 0$ and $Z < 0$ planes, respectively. Prototype of the fabricated antenna is shown in Figure 10.

There is a good matching of reflection coefficient between the measured and simulated result for proposed antenna shown in Figure 11. Corresponding computed and measured axial ratio is calculated

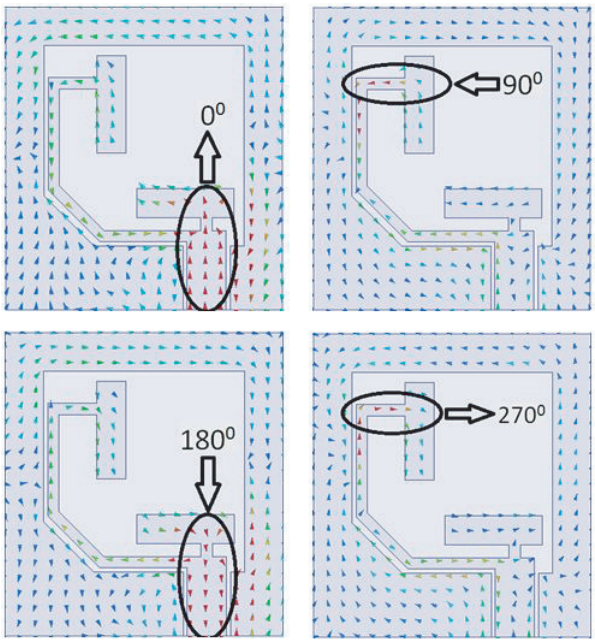

Figure 9. Current distribution plot of the antenna at different time instants.

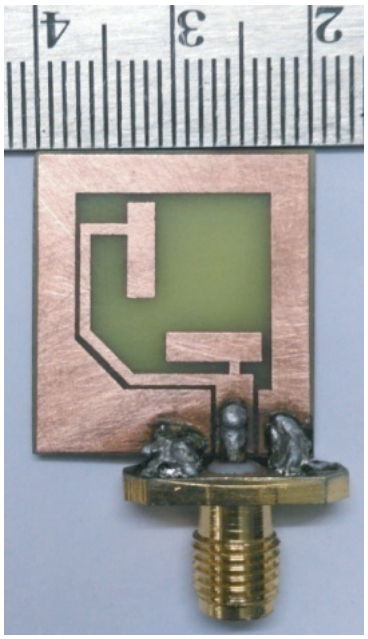

Figure 10. Photograph of the fabricated antenna.

at bore sight ($\theta = 0°$, $\varphi = 0°$) of the designed antenna. The circularly polarized antenna under test (AUT) (also referred to as receiving antenna) is kept fixed about its electrical boresight direction and rotates the source antenna. The difference between the maximum and minimum received signal levels is a direct indication of the AUT's axial ratio. If axial ratio is less than 3 dB, then the antenna can be considered as a CP antenna at that particular frequency. Figure 12 shows the measured value of the CP bandwidth (AR $\leq$ 3). Compared with Ant 3, broader CP bandwidth is achieved after the modification of the square slot on the ground plane. The measured 3 dB AR bandwidth of the proposed one is 520 MHz (4.85–5.37 GHz), which is much wider than Ant 3 having only about 300 MHz (4.76–5.06 GHz) 3 dB AR bandwidth.

At each frequency point, gain is measured by using the FRIIS Transmission equitation which is

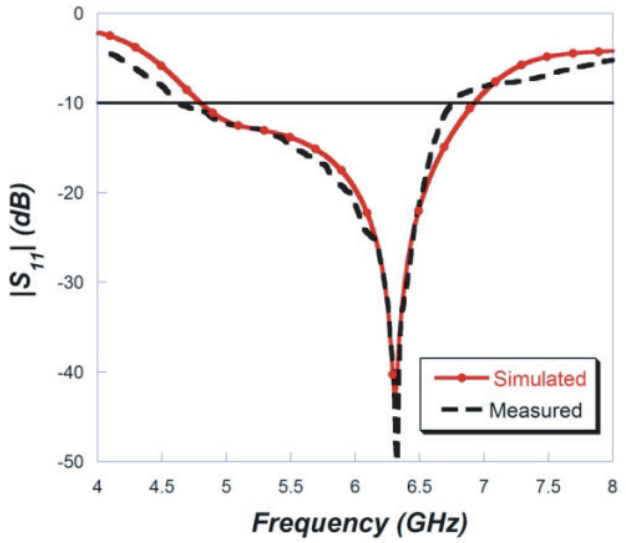

Figure 11. Simulated and measured S_{11} values for the proposed antenna.

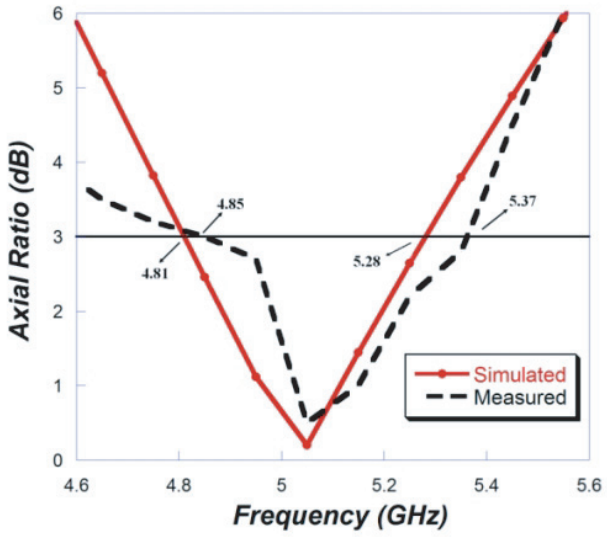

Figure 12. Simulated and measured axial ratio values for the proposed antenna.

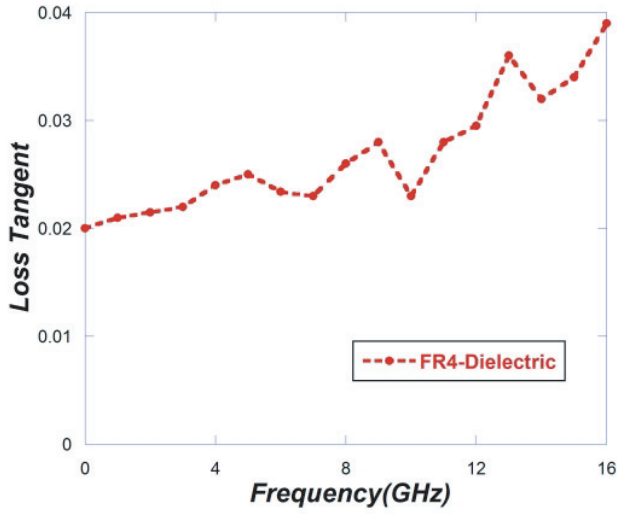

Figure 13. Dielectric loss tangent of FR-4 substrate materials.

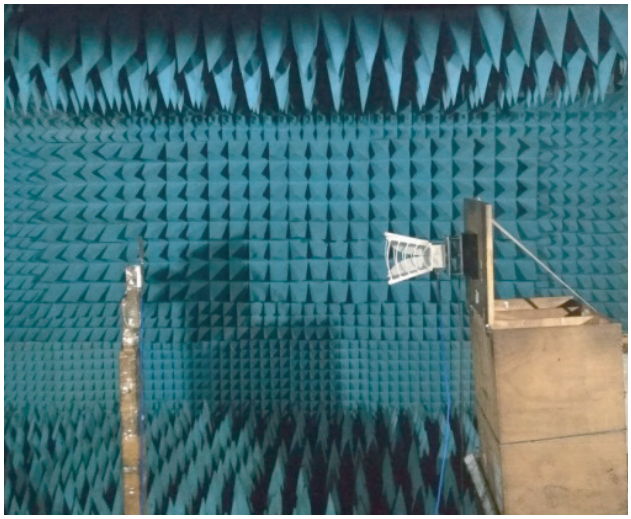

Figure 14. Experimental setup.

given as,

$$P_{\text{AUT}} = P_{\text{ref}}\,(\text{dBm}) + G_{AUT}\,(\text{dB}) + G_{ref}\,(\text{dB}) + 20\log_{10}\left(\frac{\lambda}{4\pi R}\right)$$

Here, P_{ref} denotes the power transmitted by the reference antenna. Magnitude of the reference antenna is provided by the signal generator connected to it. P_{AUT} is the power received by the antenna under test (AUT), and this is read from the power meter connected with the AUT. G_{ref} and G_{AUT} are the gain of the reference antenna and the AUT, respectively. λ is the wavelength of the transmitted signal and R the distance between two antennas. Two identical horn antennas for the desired frequency range are used at first. One will act as the reference antenna and the other as AUT. The antennas are oriented face to face in E-plane. P_{ref} is set from the signal generator, and the corresponding P_{AUT} is measured from the power meter. Since the antennas are identical, the values of G_{ref} and G_{AUT} are equal. Hence, from this setup, the gain of the horn antenna is calculated by using the above equation. Next, the horn as P_{AUT} is replaced with the fabricated antenna in its E-plane. Using the same P_{ref}, the corresponding

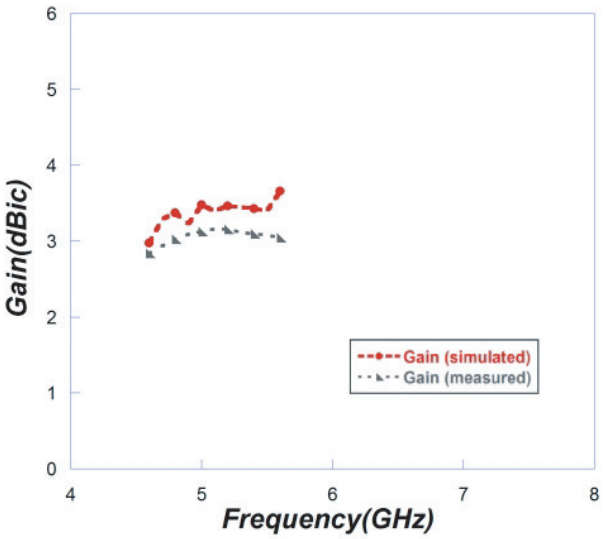

Figure 15. Simulated and measured gain.

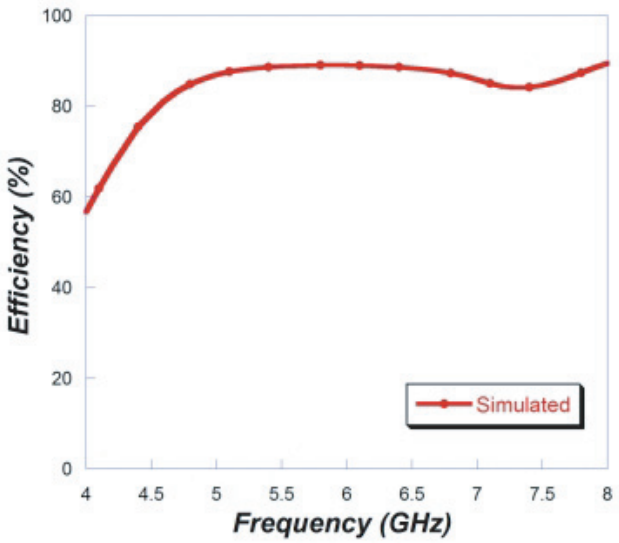

Figure 16. Efficiency plot for the proposed antenna.

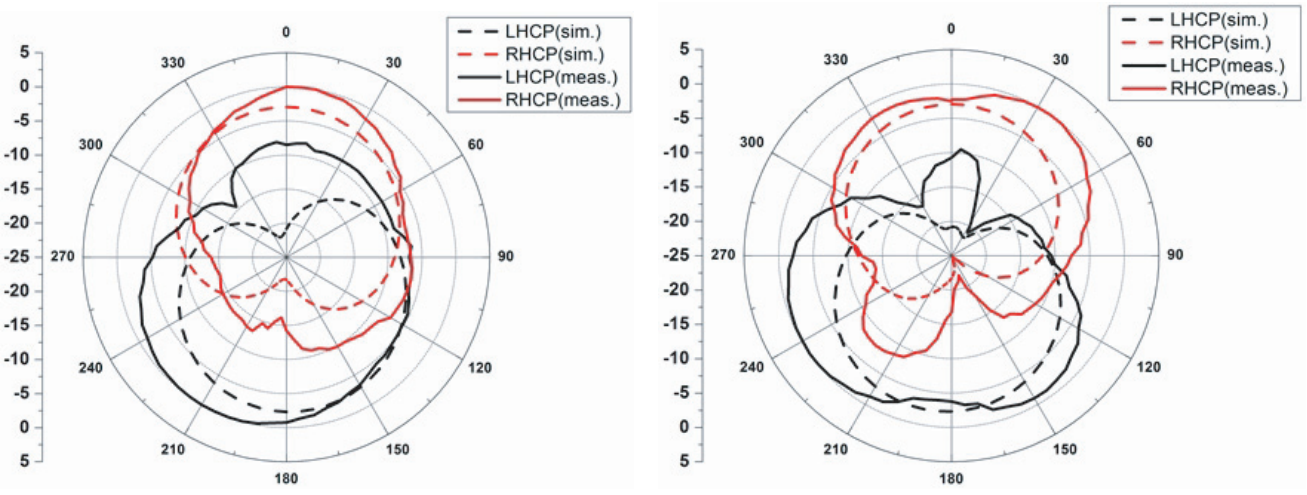

Figure 17. Radiation pattern plot-at 5.2 GHz. (a) XZ plane. (b) YZ plane.

P_{AUT} is read from the power meter. In this case, G_{ref} is the gain of the horn antenna which we got in the previous step. Now, by using the above equation, G_{AUT} is calculated. Figure 14 shows the experimental setup for measuring the proposed antenna.

The gain variation within CP bandwidth against frequency is shown in Figure 15, and the variation is less than 0.4 dBic within the whole CP bandwidth. Maximum gain obtained within the CP bandwidth is 3.12 dBic around 5.2 GHz. The discrepancy between simulated and measured gains occurs due to tolerances in the dielectric constant and loss tangent of the substrate. As the loss tangent increases with frequency, antenna gain decreases. Every unit step (i.e., $1e^{-3}$) increase in loss tangent results in 0.99% loss in antenna gain [28]. Variation of loss tangent as a function of frequency is shown in Figure 13. VSWR value of the proposed antenna is less than 2 dB in the entire impedance bandwidth.

The antenna shows a good efficiency in the entire CP bandwidth which is greater than 80% as shown in Figure 16. RHCP and LHCP radiation pattern of the proposed antenna at 5.2 GHz is shown in Figure 17. A good separation is observed between RHCP and LHCP components of the antenna. At 5.2 GHz, the antenna behaves as an RHCP antenna in $Z > 0$ direction.

4. CONCLUSION

A novel CPW-fed circularly polarized antenna with enhanced CP bandwidth is designed, fabricated and configured at *4.9 GHz (802.11j) WLAN for public safety* and *WLAN (U-NII-1 and U-NII-2A) ranging from 5.150 to 5.350 GHz for indoor use*. The proposed design has a compact dimension of $0.37\lambda_0 \times 0.34\lambda_0 \times 0.012\lambda_0\,\mathrm{mm}^3$ which is simple to be fabricated on a less expensive FR-4 substrate. A wide IBW of 2.07 GHz from 4.65 to 6.72 GHz for $|S_{11}| < -10$ dB and ARBW from 4.85 to 5.37 GHz has been achieved. The results for return loss, axial ratio, far-field LHCP-RHCP radiation patterns, and gain of the proposed antenna are investigated and discussed. This structure has the advantages of simple design and compact size. This is applicable to modern wireless communications.

ACKNOWLEDGMENT

The authors would like to acknowledge IIT Kanpur for providing measurement facilities.

REFERENCES

1. Gao S, Q. Luo, and F. Zhu, *Circularly Polarized Antennas*, Wiley, West Sussex, UK, 2014.
2. Balanis, C. A., *Antenna Theory Analysis and Design*, Wiley, Hoboken, NJ, USA, 2005.
3. Babakhani, B., S. K. Sharma, and G. Mishra, "Wideband circularly polarized his backed fan-shaped antenna with directional patterns covering L1–L5 gps bands," *Microw. Opt. Technol. Lett.*, Vol. 59, 497–500, 2017.
4. Chandu, D. S. and S. S., Karthikeyan, "A novel broadband dual circularly polarized microstrip-fed monopole antenna," *IEEE Trans. Antennas Propag.*, Vol. 65, 1410–1415, 2017.
5. Sadeghi, P., J. Nourinia, and C. Ghobadi, "Square slot antenna with two spiral slots loaded for broadband circular polarisation," *IEEE Electronics Lett.*, Vol. 52, 787–788, 2016.
6. Xu, R., J. Y. Li, J. J. Yang, K. Wei, Y. X. Qi, "A design of U-shaped slot antenna with broadband dual circularly polarized radiation," *IEEE Trans. Antennas Propag.*, Vol. 65, 3217–3220, 2017.
7. Lai, X. Z., Z. M. Xie, Q. Q. Xie, and X. L. Cen, "A dual circularly polarized RFID reader antenna with wideband isolation," *IEEE Antennas And Wireless Propagation Lett.*, Vol. 12, 1630–1633, 2013.
8. Yang, F. and Y. R. Samii, "A reconfigurable patch antenna using switchable slots for circular polarization diversity," *IEEE Microw. and Wireless Components Lett.*, Vol. 12, 96–98, 2002.
9. Zhao, G., L. N. Chen, and Y. C. Jiao, "Design of a broadband dual circularly polarized square slot antenna," *Microw. Opt. Technol. Lett.*, Vol. 50, 2639–2642, 2008.

10. Zhang, C., X. Liang, X. Bai, J. Geng, and R. Jin, "A broadband dual circularly polarized patch antenna with wide beamwidth," *IEEE Antennas and Wireless Propagation Lett.*, Vol. 13, 1457–1460, 2014.
11. Jiang, L. T., S. X. Gong, T. Hong, and W. Jiang, "Broadband CPW-fed slot antenna with circular polarization," *Microw. Opt. Technol. Lett.*, Vol. 52, 2111–2114, 2010.
12. Wong, K. L., J. Y. Wu, and C. K. Wu, "A circularly polarized patch-loaded square-slot antenna," *Microw. Opt. Technol. Lett.*, Vol. 23, 363–365, 1999.
13. Jeevanandham, N., Nasimuddin, K. Agarwal, and A. Alphones, "Dual-band circularly polarized hexagonal-slot antenna," *European Microwave Conference (EuMC 2012)*, Amsterdam RAI, The Netherlands, Oct. 29–Nov. 02, 2012.
14. Nasimuddin, A. Alphones, and N. Jeevanandham, "Circularly polarized slot antennas with wideband performance," *Asia-Pacific Microwave Conference (APMC 2015)*, Nanjing, China, Dec. 06–Dec. 09, 2015.
15. Chen, W. S., K. L. Wong, and C. K. Wu, "Inset microstripline-fed circularly polarized microstrip antennas," *IEEE Trans. Antennas Propag.*, Vol. 48, 1253–1254, 2000.
16. Sung, Y. J., "Circularly polarized Mercedes-Benz logo antenna for gps applications," *Microw. Opt. Technol. Lett.*, Vol. 58, 2308–2311, 2016.
17. Fairouz, M. and M. A. Saed, "A sequentially rotated, circularly polarized microstrip antenna array with reduced mutual coupling," *Journal of Electromagnetic Waves and Applications*, Vol. 36, 422–433, 2016.
18. Pourahmadazar, J. an V. Rafii, "Broadband circularly polarised slot antenna array for L- and S-band applications," *IEEE Electronics Lett.*, Vol. 48, 542–543, 2012.
19. Karamzadeh, S., V. Rafii, M. Kartal, and H. Saygin, "Compact UWB CP square slot antenna with two corners connected by a strip line," *IEEE Electronics Lett.*, Vol. 52, 10–12, 2016.
20. Chen, J. M. and J. S. Row, "A simple design for slotted patch antennas with broadband circular polarization," *Microw. Opt. Technol. Lett.*, Vol. 57, 1854–1857, 2015.
21. Deng, I. C., J. B. Chen, Q. X. Ke, J. R. Chang, W. F. Chang, and W. T. King, "A circular CPW-fed slot antenna for broadband circularly polarized radiation," *Microw. Opt. Technol. Lett.*, Vol. 49, 2728–2733, 2007.
22. Shekhawat, S. and V. Sharma, "Circularly polarized square patch microstrip antenna with Y-shaped slot for Wi-Max application," *Euro. J. Adv. Engg. Tech.*, Vol. 1, 65–72, 2014.
23. Rana, B. and S. K. Parui, "Microstrip line fed wideband circularly-polarized dielectric resonator antenna array for microwave image sensing," *IEEE Sensors Lett.*, Vol. 1, 3500604, 2017.
24. Campbell, E., "Bluetooth radio design considerations for cellular handset application," RF Global net.
25. Majidzadeh, M., J. Nourinia, and C. Ghobadi, "Compact CPW-fed antenna with circular polarization characteristics in WLAN frequency band," *Applied Computational Electromagnetics Society (ACES)*, Vol. 28, No. 10, 938–943, 2013.
26. Nasimuddin, Z. N. Chen, and X. Qing, "Symmetric-aperture antenna for broadband circular polarization," *IEEE Trans. Antennas Propag.*, Vol. 59, No. 10, 3932–3936, Oct. 2011.
27. Nasimuddin, Z. N. Chen, and X. Qing, "Wideband circularly polarized slot antenna," *European Microwave Conference (EuMC 2012)*, Amsterdam RAI, The Netherlands, Oct. 29–Nov. 02, 2012.
28. Puttaswamy, P., P. S. K. Murthy, and B. A. Thomas, "Analysis of loss tangent effect on Microstrip antenna gain," *Int. Journal of Applied Sciences and Engineering Research*, Vol. 3, No. 6, 2014.